Bending Performance of Composite Wood I-Joist/Oriented Strand Board Panel Assemblies

William G. Davids
Derek G. Rancourt
Habib J. Dagher

Abstract

This study examined the bending performance of composite I-joist/oriented strand board (OSB) structural roof panels. The 1.22-m-wide panels were fabricated from commercially available I-joists with OSB sheathing bonded to the top and bottom I-joist flanges. To provide baseline bending performance, two sets of 10 bare I-joists were tested to failure in four-point quasistatic bending. The first consisted of 4.72-m-span, 241-mm-deep joists, and the second set consisted of 7.16-m-span, 356-mm-deep joists. Two sets of 10 I-joist/OSB panels fabricated with identical I-joists of the same spans were tested in four-point bending. Results of the bend tests showed strength gains of 59 to 124 percent and stiffness gains of 79 to 115 percent on a per-joist basis for the I-joist/OSB panels. While the bare I-joists primarily exhibited bending failures, the panels predominantly failed in shear. These strength and stiffness gains and the shift in failure mode indicate that the bonded OSB sheathing significantly improved panel bending strength. A transformed section analysis predicted panel stiffness reasonably well and indicated that shear failure was the most likely panel failure mode. Finally, four specimens were tested under sustained loading equal to 55 percent of the 5 percent parametric lower tolerance limit. Two of the specimens tested under sustained loading failed in creep rupture. Results of this study indicate that the roof panels show promise for practical application as long-span, pre-insulated structural members. However, creep deformation and creep rupture need further study, as does the durability of the I-joist–OSB bond line.

Wood I-joists are widely used in modern wood-framed construction, and their structural performance has been the subject of numerous research studies. Leichti et al. (1990) presented a detailed literature review of analytical and numerical studies conducted prior to 1990 that examined the effects of materials, joints, geometry, and environmental conditions on short- and long-term performance. More recent research has focused on the effect of web openings (Guan and Zhu 2004, Morrissey et al. 2009) and lateral-torsional buckling capacity (Hindman et al. 2005).

In 2006, I-joists accounted for nearly 60 percent of new floor construction in residential, wood-framed buildings (American Forest & Paper Association [AF&PA] 2006). However, wood I-joist rafters represent a much smaller segment of new wood-framed roof construction, where trusses are the most widely used structural members due to speed of erection. When conventional rafter construction is employed, solid-sawn rafters are used more often than I-joists due to builder familiarity and the relative ease with which complex roof geometries can be achieved.

In recent years, structural insulated panels (SIPs) have made significant market advances in roof and wall construction. Fabricated from an insulating, rigid foam core and outer sheets of oriented strand board (OSB) sheathing, SIPs combine panelized construction, excellent insulation properties, and load-bearing capacity in a single unit. However, due to their relatively low bending strength, SIP clear spans are limited. Further, panel interconnections and connection of SIPs to supporting structural framing require special fasteners and care during field erection. We also note that Crowley et al. (1993) and Crowley and Parent (1994) discussed the development of an insulated, internally vented panel with OSB webs and top and bottom layers of OSB

The authors are, respectively, Professor of Civil and Environmental Engineering (william.davids@umit.maine.edu), Former Graduate Research Assistant, Dept. of Civil and Environmental Engineering (derek.rancourt@umit.maine.edu), and Professor of Civil/Structural Engineering and Director, AEWC Advanced Structures and Composites Center (habib.dagher@umit.maine.edu), Univ. of Maine, Orono. This paper was received for publication in March 2011. Article no. 11-00036.

Forest Prod. J. 61(3):246–256.

sheathing that can span farther than SIPs. However, the system of Crowley et al. (1993) is relatively difficult to fabricate because of its use of thin OSB webs, which do not provide a large surface for bonding the top and bottom OSB sheathing. Further, it relies on complex interpanel connections and nonconventional supporting members.

The development of partial composite action between sheathing panels and solid-sawn lumber and the resulting beneficial effects on strength and stiffness have seen significant study. Vanderbilt et al. (1974) and Goodman et al. (1974) developed a mathematical model for wood-joist floor systems that accounts for partial composite action between joists and sheathing and compared their model with laboratory tests of floor systems. McCutcheon (1986) developed a simplified procedure for predicting the bending stiffness of framing members where partial composite action existed between the sheathing and the solid-sawn joists. Liu and Bulleit (1993) extended this procedure to account for load-deformation nonlinearity and the prediction of ultimate capacity in their study on the overload behavior of sheathed lumber systems. Pellicane and Robinson (1997) analyzed the response of 16,000 light-frame floor systems to assess the benefits of composite action between floor sheathing and framing members, predicting a reduction in deflection of nearly 12 percent when floor sheathing was bonded to low-modulus joists with elastomeric construction adhesive. However, this prior research largely focused on flooring systems with only top plywood or OSB sheathing. The panels studied here also have OSB sheathing attached to bottom flange, which in addition to providing further gains in stiffness could significantly increase bending strength by reducing tensile stresses in the I-joist bottom flange.

Load-duration effects must be accounted for if measured gains in short-term bending strength due to composite action are to be taken advantage of in design. Chen et al. (1989) noted significantly larger increases in creep deflection for I-joists as opposed to solid-sawn beams when members were subjected to 95 percent relative humidity (RH) for more than 30 days. Leichti and Tang (1989) compared the creep performance of I-joists with solid-sawn lumber and could draw no firm conclusions on differences in performance between the two. To avoid creep rupture failures, the load level used in the long-term tests of Leichti and Tang (1989) was 33 percent of the average short-term capacity, which they noted was close to the I-joist allowable bending stress. Johnson (2003) reported field observations of excessive deflections of in-service I-joist floors where sustained humidity levels exceeding 80 percent RH existed. Wisniewski and Manbeck (2003) subjected an I-joist floor system having OSB sheathing bonded with an elastomeric construction adhesive and nails to 508 days of sustained loading at 40 percent of the total design load. Deflections stopped increasing after about 200 days, and the deflection ratio remained below about 1.8. Roeder et al. (2005) experimentally examined the creep response of I-joist and solid-sawn floor systems subjected to 40 percent of their design load for 120 days. The floors had OSB sheathing attached with nails and construction adhesive. When subjected to identical environmental conditions, the observed creep ratios of the solid-sawn floors were greater than those for the I-joist floor systems. However, the results of these studies cannot be directly applied to the I-joist/OSB panels presently under consideration: the bottom OSB layer in the panel is carrying significant tensile stress, and it therefore will contribute significantly to creep deformations and may be a factor in creep rupture.

The research reported in this article focused on the development of composite wood I-joist/OSB roof panels (see Fig. 1). The OSB top and bottom sheathing is attached to the I-joist flanges with mechanical fasteners and construction adhesive, which results in significant composite action. Insulation is preinstalled during panel fabrication. In contrast with SIPs, internal panel venting can be provided by an air gap between the top of the insulation and the top sheathing. With proper detailing of the interpanel joints, the top or bottom layer of sheathing can also serve as a shear diaphragm, and panel erection can be easily accomplished by using conventional equipment, hardware, and fasteners. To date, two demonstration projects have been built on the University of Maine campus using these composite wood I-joist/OSB panels (see Fig. 2). The first demonstration project was a 56-m^2 roof addition (Fig. 2a), and the second project was the roof of a new, 18.29 by 33.53-m, steel-framed office and classroom facility (Fig. 2b). These demonstration projects indicate the potential utility of a rapidly erected, easily connected, pre-insulated, long-span structural roof panel. However, neither of the designs accounted for the potentially significant increases in bending stiffness and strength achieved by composite action between the top and bottom OSB sheathing and the I-joists.

The objective of this study was to assess the bending performance of the composite wood I-joist/OSB panels shown in Figure 1. Four-point bend tests were conducted on two sets of 10 nominally identical composite panels, with each set having a different span length and depth, to assess the short-term bending strength and stiffness. Additionally, tests of bare I-joists were performed to determine I-joist strength and stiffness under the same laboratory conditions. These independent bare I-joist tests allowed the stiffness and strength gains achieved by composite action between the OSB and I-joist flanges to be quantified. A transformed section analysis of the panels was conducted to assess its ability to predict composite panel stiffness and expected failure mode. Additionally, four specimens were subjected to sustained loading to assess panel performance under sustained loads.

Materials and Methods

Panel specimen fabrication

As shown in Figure 1, each panel specimen was 1.22 m wide and contained four equally spaced ALLJOIST series I-

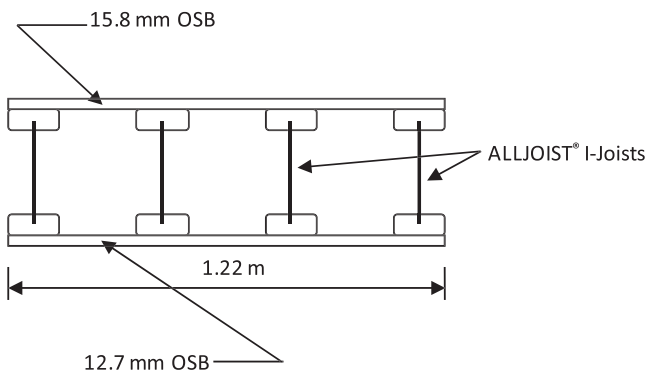

Figure 1.—Panel details. OSB = oriented strand board.

(a) UMaine Child Study Center (b) UMaine Student Innovation Center

Figure 2.—Demonstration project construction.

Joists with solid-sawn flanges and OSB webs produced by Boise Cascade (2006). We note that in a construction application, the top and/or bottom sheathing will be offset by one-half the joist flange width to allow adjoining panel edges to be interconnected in the field after placement. This detail was omitted from the panels fabricated for this testing program for simplicity and to maintain symmetric bending of the panels under transverse loading. A nominal joist spacing of 406 mm is typical of roof or floor construction. However, unlike conventional construction with individually placed rafters, the joists would be doubled at the panel edges after panel placement. This inclusion of one joist at each panel edge also led to an actual joist spacing that was slightly less than the nominal value of 406 mm. Our experience with the erection of the two demonstration projects discussed earlier indicates that joists are needed at the panel edges to provide support to the sheathing at each edge of the panel during shipping and panel placement. Insulation was not placed in the test specimens. Conventional fiberglass bat insulation, which was used in the aforementioned demonstration projects, will have no effect on panel bending strength and stiffness. However, spray foam insulation such as expanded polystyrene may increase bending strength and stiffness.

The 10 panels in the first set were 4.88 m long and fabricated from 241-mm-deep AJS-20 joists spaced at 385 mm on center. The 10 panels in the second set were 7.32 m long and fabricated from 356-mm-deep AJS-25 joists spaced at 377 mm on center. I-joists were stored away from direct moisture, and flange moisture contents (MCs) measured with a resistance meter at multiple locations along each joist varied from 8.6 to 10.3 percent. I-joist flanges were bonded to the OSB sheathing with Loctite PL Premium polyurethane construction adhesive and mechanical fasteners. Polyurethane construction adhesive was chosen based on initial tests showing that it produced a bond quality similar to that of brush- or spray-on polyurethane adhesives typically used in large-scale industrial applications, yet it had a much longer open assembly time and was easier to apply (Rancourt 2010).

The 15.8-mm-thick top and 12.7-mm-thick bottom sheathing was donated by Huber Engineered Woods and produced in 4.88-m lengths for this project by the Huber facility in Easton, Maine. The unmarked sheathing was fabricated to the same standards as the commercially available Huber AdvanTech sheathing. As detailed by Rancourt (2010), four-point bend tests were performed on OSB coupons per ASTM D3043 (ASTM International 2005b) method B to establish the modulus of elasticity (MOE) and modulus of rupture (MOR). All OSB specimens were conditioned at 65 percent RH and 21°C until an equilibrium MC of about 8.7 percent was achieved, and testing took place in a separate environmentally controlled testing facility. The OSB coupon tests established that the 12.7-mm OSB had a mean MOE of 7,950 MPa (coefficient of variation [CV] = 15.1%) and a mean MOR of 31.7 MPa (CV = 15.0%) based on tests of 13 specimens, and the 15.8-mm OSB had a mean MOE of 8,208 MPa (CV = 7.4%) and a mean MOR of 34.1 MPa (CV = 11.6%) based on tests of 15 specimens.

Panels were fabricated using spacer jigs to align the joists, and tension bridging was installed 203 mm from the end of each joist to give additional lateral support. Web stiffeners were installed at the locations of support and applied loads. A single 4.88-m-long sheet of OSB was used in the center of each panel to ensure that there were no butt joints in the top and bottom sheathing located within the region of maximum moment during the four-point bending tests. Figure 3 illustrates the procedure used to attach the sheathing. First, a 6.4-mm-wide bead of PL Premium polyurethane construction adhesive was applied using caulk guns along each joist flange contact surface (Fig. 3a). Following this, the sheathing was aligned on top of the braced joists, and the 8d pneumatic nails (60 mm long by 3-mm shank diameter) were driven through the sheathing at 305 mm on center to rapidly clamp the adhesive (Fig. 3b). After nail installation, #8 by 63.5-mm-long DuraSpin exterior wood screws were installed via a screw gun at 305 mm on center to provide additional mechanical attachment between each joist and the sheathing (Fig. 3c).

I-joist bend tests

To provide baseline strength and stiffness information for the joists used in panel fabrication, two sets of 10 I-joists were tested to failure individually in four-point quasistatic bending per ASTM D5055 (ASTM International 2004). The first set of joists consisted of 4.88-m-long (4.72-m-span), 241-mm-deep AJS-20 joists, and the second set consisted of 7.32-m-long (7.16-m-span), 356-mm-deep AJS-25 joists. These joist types, depths, and spans were identical to those used in the panel tests described later. As shown in Figure 4, load was introduced with a hydraulic actuator and a steel

Figure 3.—Panel fabrication. OSB = oriented strand board.

spreader beam. Wooden load heads with a 406-mm radius were used to apply loads at the third points of the span, and 6.4-mm-thick neoprene rubber pads were sandwiched between the load heads and test specimens and between the test specimens and end supports to reduce stress concentrations. Web stiffeners made from dimension lumber were installed in each joist at points of loading and the supports.

To accurately establish I-joist stiffness and strength, it was essential to maintain lateral stability of the I-joist compression flange during each test. Lateral stability calculations were performed per the National Design Specification for Wood Construction (NDS; AF&PA 2005), which indicated a required compression flange brace spacing of approximately 460 mm within the load span. This spacing was increased to 610 mm over the load span based on the I-joist test results reported by Hindman et al. (2005), which showed that the NDS specifications for bracing against lateral-torsional buckling are typically conservative. Bracing spacing was increased to 914 mm between the load heads and supports. Full details of the bracing calculations are given in Rancourt (2010). The lateral supports were fabricated from lumber and OSB and faced with polytetrafluoroethylene (PTFE)–impregnated plastic sheets adjacent to each compression flange to minimize friction between the lateral support and the joist flange when they came into contact. The lateral support frames were bolted to the reaction floor, and an initial clear spacing of about 1.5 mm was set between each PTFE-impregnated contact surface and joist compression flange.

Figure 4.—I-joist specimen in four-point bend setup.

Each specimen was instrumented with pairs of string potentiometers at midspan and the third points, and linear variable displacement transducers (LVDTs) at the supports. Testing was performed in displacement control, with a displacement rate selected to fail the specimen in approximately 10 minutes.

Panel bend tests

The 20 I-joist/OSB panels were tested in four-point bending per ASTM D198 (ASTM International 2005a). The 4.88-m-long panels with 241-mm-deep AJS-20 joists were tested with a 4.72-m simple span, and the 7.32-m-long panels fabricated with 356-mm-deep AJS-25 joists were tested with a 7.16-m simple span. As shown in Figure 5, the panel ends were supported by concrete barriers with 6.4-mm-thick neoprene rubber pads sandwiched between the panels and the concrete. Curved steel load heads of the same width as the panel and having a radius of 711 mm were used to distribute load across the panel width. Neoprene rubber pads were sandwiched between the load heads and the panel face. Loads were applied with a hydraulic actuator and recorded with an electronic load cell. The tests were run in displacement control, with load rates of 5 mm/min and 6.6 mm/min for the shorter and longer panels, respectively, giving a time to failure of approximately 10 minutes.

Midspan and load point deflections were measured on each side of the panels using 635-mm stroke string potentiometers. The string pots were mounted to aluminum brackets attached to the outer I-joist webs at the middepth of the panel. At each support, LVDTs were attached to the outer I-joist webs on each side of the panel in the same manner as the string pots. For each string pot and LVDT,

Figure 5.—Panel in four-point bend setup.

measurements were taken relative to frames mounted to the floor adjacent to the specimen. Reported displacements at midspan are the average values determined from the pair of string pots at midspan minus the average measured support displacements.

Panel creep tests

To assess the effect of load duration, two 4.72-m-span and two 7.16-m-span panels were subjected to sustained loading. The creep test specimens were nominally identical to the quasistatic bend test specimens. As noted in the previous review of prior creep testing, load levels used during creep tests have ranged from 40 percent of the allowable design load (Roeder et al. 2005) to 33 percent of the ultimate capacity (Leicthi and Tang 1989), and various durations of load have been considered. The load level used in the present study was 55 percent of the 5 percent lower tolerance limit, which is the load required by ASTM D6815 (ASTM International 2005c), a standard designed to assess load duration and creep effects in wood and wood-based products. For the 4.72-m-span specimens, a load of 69.4 kN was applied, and 82.4 kN was applied to the 7.16-m-span specimens; these values are 46 to 47 percent of the average short-term capacities for the two panel types.

The test period specified by ASTM D6815 (ASTM International 2005c) is 90 days, during which time specimen MCs shall not deviate more than ± 2 percent. Staying in this tight range of MCs would require that the specimens be tested in a temperature- and humidity-controlled environment. However, this was not possible due to the large specimen size, the long test duration, and the lack of available space. The first 4.72-m-span specimen (designated C1) was tested indoors beginning in April 2009 in a large manufacturing facility that, while heated in the winter, is not humidity controlled. The second 4.72-m-span specimen (C2) and the two 7.16-m-span specimens (C3 and C4) were tested outdoors beginning in May 2009. A mono-slope roof shelter was constructed and rolled over specimens C2 to C4 immediately after loading to ensure they were never subjected to direct moisture. I-joist flange MCs were measured with a resistance moisture meter at the start and end of each test. Over the test duration, the MC of the specimens increased by 1.5 to 4 percent.

All specimens were loaded in four-point bending with concrete blocks and sandbags that rested on a wood loading platform supported at the third points of the panel (see Fig. 6). The panels were supported by heavy wood blocking while the weights were being placed on the panels. To ensure that the weight was applied gradually over approximately 1 minute as specified by ASTM D6815, hydraulic jacks were used to allow removal of the blocking and controlled application of the load. Displacements were measured at the supports and midspan using dial gages which indicated displacement to the nearest 0.00004 mm. Dial gages were mounted on separate frames on each side of the panels at midspan and the supports.

Displacements were made relative to the top of the panels. RH was also monitored for each specimen during the testing period using hygro-thermometers located inside the shelters. The hygro-thermometers reported maximum and minimum levels since the last reading, and readings of environmental conditions were taken in conjunction with deflection readings.

Figure 6.—Creep test prior to sheltering specimen.

Results and Discussion

I-joist bend tests

Figures 7 and 8 show the measured midspan load-displacement response for the 241-mm-deep I-joists and 356-mm-deep I-joists, respectively. All of the 241-mm-deep joists failed in tension at a lower flange finger joint. For the 356-mm-deep joists, 7 of 10 specimens failed in tension in the lower flange, two specimens exhibited a flange compression failure, and one specimen failed in web shear. Figure 9 shows the three observed failure modes. Shear failure tended to occur at web knock-out holes as shown in Figure 9c, or at the web tongue and groove joints between individual pieces of sheathing.

The mean ultimate moment capacity and flexural rigidity, *EI,* for the 241-mm joists were 12.85 kN·m and 752.2 kN·m^2, respectively, and corresponding CVs in strength and stiffness were 15.5 and 3.9 percent. The mean ultimate moment capacity and *EI* for the 356-mm joists were 33.3 kN·m and 2,520 kN·m^2 with CVs in strength and stiffness of 24.4 and 6.5 percent. The *EI* values were computed from only the flexural deflections. Shear deflections were estimated using the shear deflection coefficient *K* published by the joist manufacturer and represented approximately 10 percent of the total deflection as detailed by Rancourt (2010).

The larger variability in the strength results for the 356-mm I-joists likely reflects the fact that only 7 of 10 of the 356-mm joists failed in flange tension. If the three specimens that failed in either compression or shear are ignored, the mean ultimate moment capacity and *EI* for the 356-mm joists become 29.23 kN·m and 2,426 kN·m^2 with corresponding CVs of 3.0 and 19.8 percent, respectively. Overall, however, both sets of specimens showed high variability in strength results, which is likely due to the small sample size.

To put the strength and stiffness results in perspective, the allowable moment capacities can be computed and compared with published values. Due to the small sample size, this requires the use of parametric statistics based on the 5 percent parametric tolerance limit (5% PTL) given in Equation 1.

$$5\%\,\mathrm{PTL} = \bar{x} - ks \tag{1}$$

where $\bar{x}$ is the sample mean, s is the sample standard deviation, and k is a function of the confidence and sample size. ASTM D5055 (ASTM International 2004) specifies

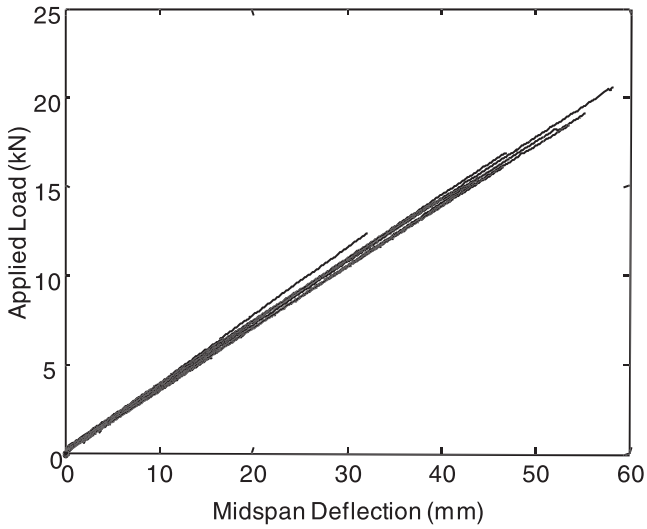

Figure 7.—Load deflection of 241-mm I-joists.

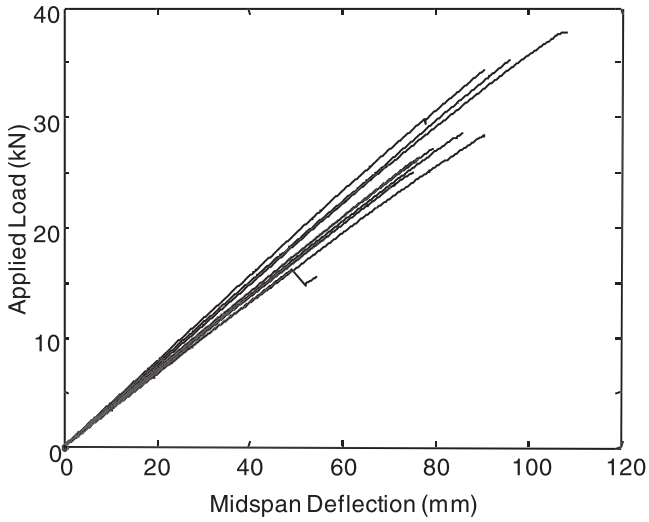

Figure 8.—Load deflection of 356-mm I-joists.

that the bending strength M_{all} of wood I-joists shall be computed with 75 percent confidence and divided by 2.1 to provide an additional factor of safety and account for load-duration effects. Table 1 compares the computed and published values of the joist allowable moment capacity and *EI,* where the subscript ''pub'' denotes the manufacturer-published values. The percent differences are relative to the experimentally determined values. For both sets of joists, the allowable bending strengths derived from the test data reported here are lower than the published allowable strengths. This may be due to the small sample size and the use of parametric statistics.

Table 1.—Comparison of allowable joist bending strength and stiffness.[a]

Joist depth (mm)	M_{all} (kN·m)	M_{pub} (kN·m)	% diff in M_{all}	EI (kN·m^2)	EI_{pub} (kN·m^2)	% diff in EI
241	4.12	4.61	10.5	752.2 (3.9%)	631.6	−16.0
356	7.71	10.2	24.3	2,520 (6.5%)	2,179	−13.5

[a] M_{all} = allowable bending strength derived from joist testing; M_{pub} = manufacturer-published allowable bending strength; EI = flexural rigidity derived from joist testing; EI_{pub} = manufacturer-published flexural rigidity. Values in parentheses are coefficients of variation.

Panel bend tests

Figures 10 and 11 present the measured load-displacement response at the panel midspan for the 4.72- and 7.16-m-span panels. Additionally, Tables 2 and 3 contain detailed strength, displacement, and stiffness results for both sets of panels. In contrast with the bare I-joist test results, 80 percent of the 4.72-m-span and 70 percent of the 7.16-m-span panels failed in shear, with the remaining panels failing in bending. Figure 12 shows typical shear and bending failures. The shear failures (Fig. 12a) were generally characterized by a diagonal web crack centered between a load head and support. The bending failures (Fig. 12b) occurred in panels where manufactured finger joints in the I-joist tension flanges were unintentionally located in the same position within the span in adjacent joists. The predominance of shear failures indicates that the OSB provided significant additional bending capacity to the cross section through composite action. Also of interest is the smaller variability in strength when compared with the plain I-joists: the CV in capacity was 6.6 percent for the 4.72-m-span panels, and 7.4 percent for the 7.16-m-span panels. This sharp reduction in strength variability may be due to the presence of the bonded OSB carrying significant tensile bending stresses and thus reducing the significance of strength-limiting defects in the I-joist tension flange such as splices and knots.

Table 4 compares the ultimate capacity and flexural stiffness of the panels with the bare I-joists. Due to the large number of shear failures in the panels, ultimate capacities are reported as loads and not bending moments. Percent increases are based on comparing one-fourth of the average panel strength and stiffness values given in Tables 2 and 3 with the strength and stiffness of a single joist of the same

Figure 9.—I-joist failure modes.

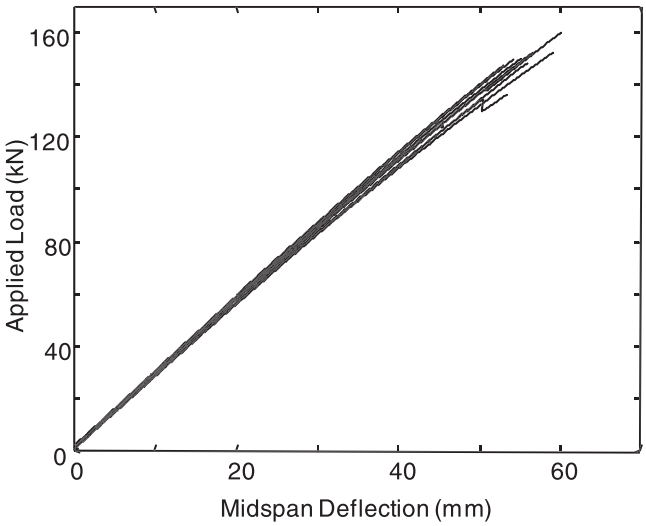

Figure 10.—Load deflection of 4.72-m-span panels.

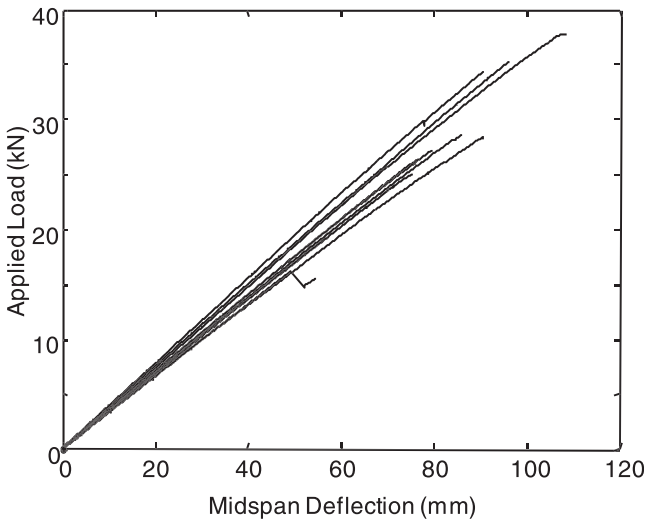

Figure 11.—Load deflection of 7.16-m-span panels.

type and span. The results in Table 4 clearly show that bonded OSB sheathing significantly increases strength and stiffness on a per-joist basis. There is a marked difference in the increase between joist types, however, with the 7.16-m-span (356-mm I-joist) panel specimens experiencing an average increase in strength of 59 percent compared with a 124 percent increase in strength for the 4.72-m-span (241-mm I-joist) panels. This is attributed to the thickness and width of the OSB sheathing tributary to each joist remaining constant. It follows that as the joist depth and strength increase, the relative benefit provided by the bonded OSB sheathing will decrease.

Analysis of panel short-term bending response

To examine the panel bend test results more closely and help explain observed response, a transformed section analysis of the panel was performed. In these analyses, the joists were considered to be made from a single material, and the joist *EI* was taken as the average value determined from the joist bend tests. In reality, of course, the joist OSB webs have a much lower MOE than the flanges, and a more accurate analysis would account for the different material properties of the joist web and flanges. However, the contribution of the web to the overall moment of inertia of the joist is quite small, so the error inherent in considering the joists to be homogeneous is also small. The MOE of the top and bottom layers of OSB was taken as the MOE determined from the OSB coupon tests when computing the transformed section properties. For details on the transformed section method of analysis, see a standard mechanics of materials text such as Gere and Timoshenko (1984).

The MOE of the uniform bare I-joist, E_j, was computed from Equation 2:

$$E_j = \frac{EI_j}{I_j} \tag{2}$$

where EI_j is the average joist flexural rigidity determined from the I-joist bend tests, and I_j is the cross-sectional moment of inertia computed from published joist dimensions. This calculation yields E_j = 13.9 GPa for the 241-mm-deep joists, and E_j = 13.3 GPa for the 356-mm-deep

Table 2.—Results of static panel bend tests for 4.72-m-span specimens.[a]

Specimen no.	MC (%)	P_{ULT} (kN)	Δ_{ULT} (mm)	EI_{FLEX} (kN·m²)	M_{ULT} (kN·m)	Failure mode[b]
1	10.2	159.9	60.20	6,468	125.9	S
2	10.3	140.3	53.34	6,457	110.5	S
3	9.1	126.2	45.47	6,589	99.4	S
4	10.2	148.2	56.13	6,259	116.7	S
5	9.5	149.9	54.36	6,612	118.1	S
6	9.8	152.6	59.44	6,247	120.2	S
7	9.6	147.8	53.09	6,692	116.4	M
8	9.6	150.0	55.37	6,529	118.1	S
9	9.5	136.5	53.59	6,356	107.5	S
10	9.3	152.5	56.90	6,437	120.1	M
Average	9.7	146.4	54.79	6,465	115.3	
SD	0.4	9.6	4.10	147	7.6	
CV (%)	4.2	6.6	7.5	2.3	6.6	

[a] MC = moisture content; P_{ULT} = specimen ultimate load; Δ_{ULT} = displacement corresponding to ultimate load; EI_{FLEX} = flexural rigidity derived from panel test; M_{ULT} = specimen ultimate moment; CV = coefficient of variation.
[b] S = web failure due to shear; M = flange failure due to moment.

Table 3.—Results of static panel bend tests for 7.16-m-span specimens.[a]

Specimen no.	MC (%)	P_{ULT} (kN)	Δ_{ULT} (mm)	EI_{FLEX} (kN·m^2)	M_{ULT} (kN·m)	Failure mode[b]
1	9.2	187.3	81.03	18,604	223.8	S
2	9.2	178.9	79.50	18,150	213.6	S
3	9.1	159.3	69.60	18,153	190.3	M
4	9.4	193.1	85.60	17,989	230.3	S
5	9.6	151.7	70.10	17,504	180.9	S
6	9.1	183.3	78.49	18,343	218.8	M
7	9.0	186.9	86.11	17,295	223.3	S
8	9.7	176.2	81.79	16,913	210.4	M
9	9.4	173.1	73.15	19,032	206.6	S
10	8.6	186.5	80.52	18,380	222.6	S
Average	9.2	177.6	78.59	18,036	212.1	
SD	0.3	13.2	5.86	637	15.7	
CV (%)	3.4	7.4	7.5	3.5	7.4	

[a] MC = moisture content; P_{ULT} = specimen ultimate load; Δ_{ULT} = displacement corresponding to ultimate load; EI_{FLEX} = flexural rigidity derived from panel test; M_{ULT} = specimen ultimate moment; CV = coefficient of variation.
[b] S = web failure due to shear; M = flange failure due to moment.

Figure 12.—Panel failure modes.

joists. These values agree reasonably well with the published joist flange modulus of 12.4 GPa (International Code Council Evaluation Service [ICC-ES] 2003).

Next, the top and bottom layers of OSB sheathing were transformed to an equivalent width of joist material by dividing the panel width of 1.22 m by the ratio n defined in Equation 3:

$$n = \frac{E_j}{E_{OSB}} \quad (3)$$

where E_{OSB} is the MOE of the OSB sheathing determined from the previously described OSB coupon tests. The full 1.22-m width of both the top and bottom panels was assumed to be effective. Given the transformed section, the flexural rigidity EI_p was computed for the 4.72-m-span panels as 7,590 kN·m^2 and as 19,700 kN·m^2 for the 7.16-m-span panels. These computed EI_p values exceed the measured panel EI_{FLEX} values by 17.3 and 9.2 percent, respectively. One possible reason for this discrepancy is the assumption that the full 1.22-m width of the top and bottom sheathing is effective. It is well known that shear lag effects can reduce effective flange width; this is taken into account in the design of concrete T-beams (American Concrete Institute 2008) and the design of steel beams with composite concrete decks (American Institute of Steel Construction 2006). For example, reducing the OSB flange width by 20 percent (from 1.22 to 0.976 m) results in EI_p values for the 4.72- and 7.16-m-span panels of 6,680 and 17,800 kN·m^2, respectively, which are 3.2 percent above and 1.5 percent below, respectively, the experimentally derived EI_{FLEX} values.

Table 4.—Comparison of bare joist and composite panel mean strength and stiffness.[a]

	Set 1: 4.72-m-span specimens		Set 1: 7.16-m-span specimens	
Specimen	EI_{FLEX} (kN·m^2)	P_{ULT} (kN)	EI_{FLEX} (kN·m^2)	P_{ULT} (kN)
Bare joist	752 (3.9%)	16.3 (3.9%)	2,520 (6.5%)	27.88 (24.4%)
Panel	6,465 (2.3%)	146 (6.6%)	18,036 (3.5%)	178 (7.4%)
Panel/4	1,616	37	4,509	44
% increase	115	124	79	59

[a] EI_{FLEX} = flexural rigidity derived from joist or panel test; P_{ULT} = ultimate load from joist or panel test. Values in parentheses are coefficients of variation.

The tensile bending stress in the I-joist bottom flange at the average failure load was computed from the transformed section analysis as 30.5 GPa in the 4.72-m-span panels and 29.5 GPa in the 7.16-m-span panels. These values are quite close to the average computed stress at failure in the bare I-joists of 28.6 and 31.3 GPa for the 241- and 356-mm-deep joists, respectively. The tensile bending stresses in the bottom OSB sheathing was computed from the transformed section analysis as 19.2 and 18.8 GPa for the two sets of panel tests, which is significantly less than the MOR of 31.7 GPa determined from OSB coupon tests. The average panel shear stress at failure, computed as the shear divided by the area of the OSB web, was 11.6 GPa for the 4.72-m-span panels and 8.3 GPa for the 7.16-m-span panels. The ''Wood Handbook'' (US Department of Agriculture 1999) gives the range 6.9 to 10.3 GPa for edgewise shear strengths of sheathing grade OSB. The average panel shear stress exceeds the upper limit of this range for the shorter-span panels and falls in the middle of this range for the longer-span panels. Further, the I-joist webs have discontinuities at joints between individual OSB sheets as well as perforations for knock-out holes, both of which will tend to reduce web shear capacity.

This comparison of calculated stresses with expected capacities indicates that the panels, unlike the bare joists, were likely to fail in shear. This is consistent with the experimentally observed response, where 15 of the 20 panels tested failed in shear. We note that while the bottom joist flange tensile stress was very near the values observed during the bending failures of the bare I-joists, the majority of the bare I-joist flange tension failures occurred at finger joints or other flange defects. The bottom layer of OSB sheathing present in the panel tests likely prevented these weak flange locations from failing by bridging these defects. Overall, the good agreement between the analysis and the observed panel response shows that transformed section analysis would be an appropriate design tool for the composite I-joist/OSB panels.

Panel creep tests

Figures 13 through 16 show the measured midspan displacement and RH over the test duration for each specimen, and Table 5 summarizes critical values derived

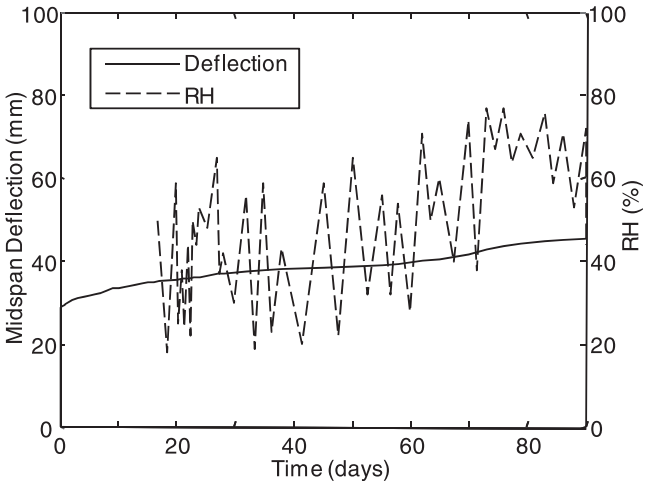

Figure 13.—Deflection and relative humidity (RH) versus time for specimen C1.

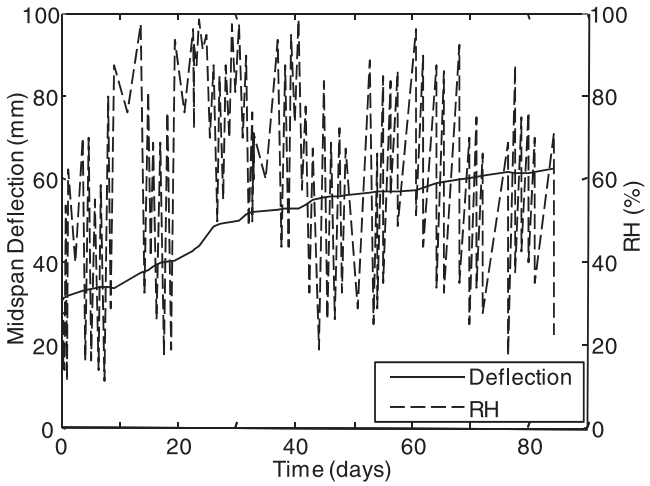

Figure 14.—Deflection and relative humidity (RH) versus time for specimen C2.

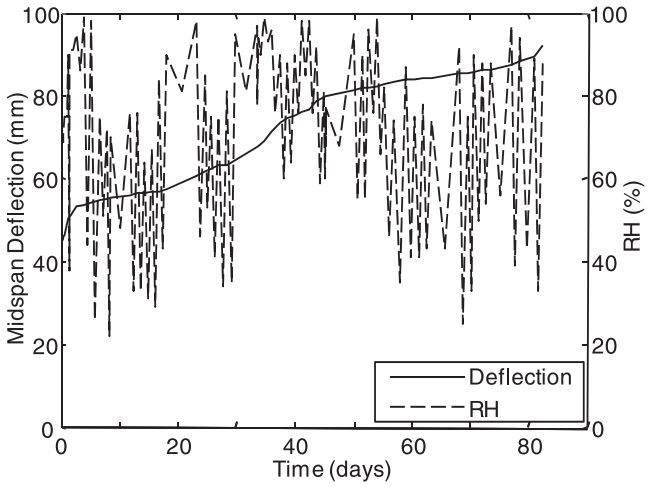

Figure 15.—Deflection and relative humidity (RH) versus time for specimen C3.

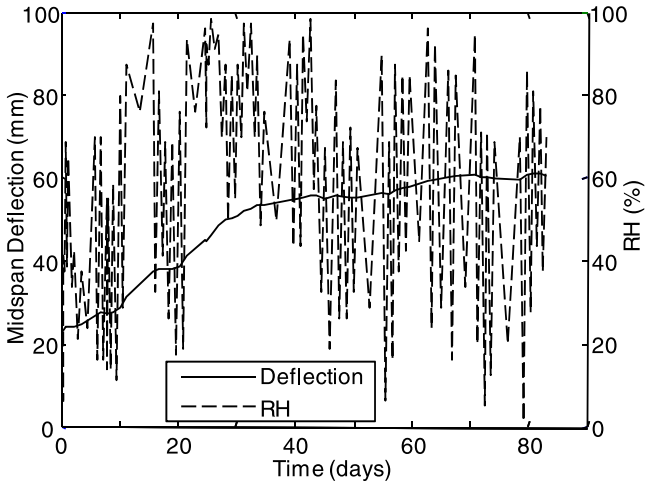

Figure 16.—Deflection and relative humidity (RH) versus time for specimen C4.

Table 5.—Summary of creep test results.[a]

Specimen ID	MC (%)		Test duration (d)	Creep rupture	D_i (mm)	D_{max} (mm)	FD_{max}
	Initial	Final					
C1	9.5	11	90	No	27.4	45.6	1.67
C2	10.0	13.5	75[b]	No	24.4	62.3	2.55
C3	9.0	13.5	64	Yes	40.0	92.2	2.31
C4	8.5	12.5	74	Yes	36.4	76.2	2.09

[a] MC = moisture content; D_i = initial deflection measured after application of full load; D_{max} = maximum recorded deflection; FD_{max} = maximum fractional deflection.
[b] Test was terminated prematurely due to loss of testing space.

from each test. In Table 5, D_i is the initial deflection recorded at application of the full load, D_{max} is the maximum measured deflection over the test duration, and FD_{max} is the maximum fractional deflection defined per Equation 4. We note here that D_i was incorrectly read for specimen C3, and the reported value is the one expected based on the average panel deflections measured in the quasistatic tests. The incorrect reading of D_i did not affect the displacements read during the test duration but did require that these later displacement readings be adjusted to reflect the new value of D_i.

$$FD_{max} = \frac{D_{max}}{D_i} \quad (4)$$

A review of Figures 13 through 16 indicates a strong correspondence between increasing creep rate and fluctuation in RH. Specimen C1, which was tested indoors and experienced the lowest overall humidity and the least change in MC of all specimens, had the lowest fractional creep deflection. Specimen C2, which was nominally identical to C1 and was tested outdoors, experienced a much more humid environment and a greater increase in flange MC and displayed much larger creep displacements. The test of specimen C2 had to be terminated at 75 days due to the loss of the testing space, and creep deflections likely would have continued to increase had it been tested for the full 90 days.

Both of the 7.16-m specimens failed in bending creep rupture prior to completion of the 90-day loading period. Specimen C3 exhibited a tensile failure of the I-joist bottom flange near midspan. The failure appeared to initiate at a finger joint and propagate up through the OSB web. Interestingly, the two sides of the flange finger joint were largely undamaged, indicating failure of the adhesive at the finger joint. Specimen C4 also failed in bending-induced tension, and failure appeared to initiate at a joist finger joint within the load span. The fact that both 7.16-m-span specimens failed in bending, while 80 percent of the quasistatically tested specimens failed in shear may be because of the greater susceptibility of the solid-sawn I-joist flange to tensile creep rupture than the OSB web to shear creep rupture. However, the authors are not aware of any prior work that has quantified the shear creep-rupture properties of OSB, and only two creep tests were performed, so this statement is speculative.

None of the specimens satisfied the ASTM D6815 (ASTM International 2005c) requirements for satisfactory creep performance, which are (1) $FD_{max} \leq 2$; (2) decreasing creep rates over the test duration; and (3) no creep rupture during the 90-day test period.

Summary and Conclusions

This study has focused on assessing the structural performance of composite I-joist/OSB structural panels. Results of quasistatic bend tests of both the structural panels and plain I-joists showed gains in strength of 59 to 124 percent and gains in stiffness of 79 to 115 percent due to composite action for the two joist–span combinations tested. A straightforward transformed section analysis of the composite panel predicted panel stiffness and panel failure mode reasonably well. However, none of the four panel specimens tested under sustained loading passed the criteria set forth in ASTM D6815 (ASTM International 2005c).

The test results and analyses indicate that the composite roof panel system shows promise for practical applications. The two demonstration projects briefly discussed here indicate that roof erection time with the panel is faster than with conventional stick-built construction. The additional material required beyond conventional roof construction is the single bottom layer of OSB sheathing and a 33 percent increase in the number of I-joists. Despite this additional required material, the benefits of rapid erection, preinstalled insulation with internal venting, and significantly higher strength and stiffness may make the panels cost-effective for the construction of simple roof geometries. However, there are several issues noted below that must be addressed before the full benefits of the panels can be realized in conventional construction.

1. Durability of the I-joist–OSB bond. The panels rely on composite action between the OSB sheathing and the I-joist. The research conducted here did not assess bond line durability, which is critical for a long-lived roof application. The use of industrial polyurethane (or other weather-resistant) adhesives needs to be investigated. Finally, the use of both nails and screws as done in this study may be unnecessary, and the required type and spacing of mechanical connectors should be optimized through further testing and analysis.
2. Performance under sustained load and creep rupture potential. Two of the four panels tested under sustained load failed in creep rupture. However, we note that ASTM D6815 (ASTM International 2005c) specifies a high sustained load relative to that which has been considered in previous studies. Further, MC fluctuations were larger than recommended by ASTM D6815 for three of the four specimens and clearly affected panel deflections. Consideration should be given to testing the panels under more realistic sustained loads or testing the panels under the requirements of ASTM E72 (ASTM International 2009), which is approved by the ICC-ES for assessing load duration effects of sandwich panels.

Ultimately, the ability of the panels to safely carry sustained loads without excessive deflection or creep rupture must be established before panel design strengths can be determined.

3. Interpanel and panel-to-wall connection details. Simple methods of field connecting adjacent panels should be developed and tested for efficacy in achieving diaphragm action. Panel-to-wall connection details need to be developed and tested.
4. Assessment of insulation alternatives. As with SIPs, the panels can be heavily insulated. The performance and cost of different insulation materials need to be assessed, and details developed for insulating between abutting I-joists in adjacent panels.
5. Extension to complex roof geometries. As presented here, the roof panels are directly applicable to simple flat or mono-sloped roof geometries, which are common in light-framed industrial structures. Use of a ridge would require tension ties to be connected to the panels or the use of a structural ridge beam. More complex geometries including hipped roofs and dormers commonly found in residential construction would require significant further research into the panel fabrication and interpanel and panel-to-structure connections.
6. Development of panel design values. Rancourt (2010) developed preliminary roof load-span tables for the composite roof panels of this study using the provisions of ASTM D5055 (ASTM International 2004) that take into account shear and bending strength as well as deflection. The load-span tables indicate that significant gains in span beyond normal I-joist construction are feasible. However, a small number of nominally identical panel specimens were tested in this study, and a definitive calculation of allowable capacities will require additional testing. As noted earlier, further assessment of creep rupture and deflection under sustained load must also be performed prior to establishing design strengths. It should also be noted that for flooring systems with multiple, solid-sawn joists spaced at less than 610 mm on center, the NDS (AF&PA 2005) allows joist capacity to be increased by a repetitive member factor that accounts for redundancy and system effects. The development of the repetitive member factor dates back to studies on load-sharing in redundant systems (DeBonis 1980). However, repetitive member factors should not be considered when computing allowable strengths for the panels considered in this study. The panels contain multiple joists but are tested as individual members; further, the NDS (AF&PA 2005) does not allow the repetitive member factor to be applied to I-joists.

Literature Cited

American Concrete Institute (ACI). 2008. Building code requirements for structural concrete (ACI 318-08) and construction requirements. ACI, Farmington Hills, Michigan.

American Forest & Paper Association (AF&PA). 2005. National design specification for wood construction. AF&PA, Washington, D.C.

American Forest & Paper Association (AF&PA). 2006. Engineered wood products primer awareness guide. AF&PA, Washington, D.C.

American Institute of Steel Construction (AISC). 2006. Manual of Steel Construction. 13th ed. AICS, Chicago.

ASTM International. 2004. Standard specification for establishing and monitoring structural capacities of prefabricated wood I-joists. ASTM D5055. ASTM International, West Conshohocken, Pennsylvania.

ASTM International. 2005a. Standard test methods of static tests of lumber in structural sizes. ASTM D198. ASTM International, West Conshohocken, Pennsylvania.

ASTM International. 2005b. Standard test methods for structural panels in flexure. ASTM D3043. ASTM International, West Conshohocken, Pennsylvania.

ASTM International. 2005c. Standard specification for evaluation of duration of load and creep effects of wood and wood-based products. ASTM D6815. ASTM International, West Conshohocken, Pennsylvania.

ASTM International. 2009. Standard test methods of conducting strength tests of panels for building construction. ASTM E72. ASTM International, West Conshohocken, Pennsylvania.

Boise Cascade. 2006. Boise Cascade ALLJOIST Specifier Guide. 10th ed. Boise Cascade, LLC, Boise, Idaho.

Chen, G., R. C. Tang, and E. W. Price. 1989. Effect of environmental conditions on the flexural properties of wood composite I-beams and lumber. *Forest Prod. J*. 39(2):17–22.

Crowley, J., J. Dentz, L. Morse-Fortier, and M. Parent. 1993. Reinventing wood frame construction: Development of an innovative roof component system. *Forest Prod. J*. 43(7/8):27–35.

Crowley, J. S. and M. R. Parent. 1994. Roof panel design and single beam roof assembly. US patent 5,365,704.

DeBonis, A. L. 1980. Stochastic simulation of wood load-sharing systems. *ASCE J. Struct. Div*. 106(ST2):393–410.

Gere, J. M. and S. P. Timoshenko. 1984. Mechanics of Materials. 2nd ed. PWS Engineering, Boston.

Goodman, J. R., M. D. Vanderbilt, M. E. Criswell, and J. Bodig. 1974. Composite and two-way action in wood joist floor systems. *Wood Sci*. 7(1):25–33.

Guan, Z. W. and E. C. Zhu. 2004. Nonlinear finite element modeling of crack behavior in oriented strand board webbed wood I-beams with openings. *J. Struct. Eng*. 130(10):1562–1569.

Hindman, D., H. B. Manbeck, and J. J. Janowiak. 2005. Measurement and prediction of lateral torsional buckling loads of composite wood materials: I-joist sections. *Forest Prod. J*. 55(10):43–48.

International Code Council Evaluation Service (ICC-ES). 2003. AJS series prefabricated wood I-joists. Report ESR-1144. ICC-ES, Whittier, California.

Johnson, A. 2003. Creep of wood I-joists exposed to abnormally high moisture conditions. *Pract. Period. Struct. Des. Construct*. 8(1):36–40.

Leichti, R. J., R. H. Falk, and T. L. Laufenberg. 1990. Prefabricated wood composite I-beams: A literature review. *Wood Fiber Sci*. 22(1): 62–79.

Leichti, R. J. and R. C. Tang. 1989. Comparative performance of long-term loaded wood composite I-beams and sawn lumber. *Wood Fiber Sci*. 21(2):142–154.

Liu, W.-F. and W. M. Bulleit. 1993. Overload behavior of sheathed lumber systems. *J. Struct. Eng*. 121(7):1110–1118.

McCutcheon, W. J. 1986. Stiffness of framing members with partial composite action. *J. Struct. Eng*. 112(7):1623–1637.

Morrissey, G. C., D. W. Dinehart, and W. G. Dunn. 2009. Wood I-joists with excessive web openings: an experimental and analytical investigation. *J. Struct. Eng*. 135(6):655–665.

Pellicane, P. J. and G. Robinson. 1997. Effect of construction adhesive and joist variability on the deflection behavior of light-frame wood floors. *J. Test. Eval*. 25(2):163–173.

Rancourt, D. 2010. Structural behavior of wood I-joist/OSB roof panel assemblies. Master's thesis. University of Maine, Orono.

Roeder, R. W., Jr., H. B. Manbeck, and J. J. Janowiak. 2005. Creep behavior of solid-sawn and wood I-joist floors. *Trans. ASAE* 48(1): 341–349.

US Department of Agriculture (USDA). 1999. Wood handbook: Wood as an engineering material. General Technical Report FPL-GTR-113. US Department of Agriculture, Forest Products Laboratory, Madison, Wisconsin.

Vanderbilt, M. D., J. R. Goodman, and M. Criswell. 1974. Service and overload behavior of wood floor joist systems. *ASCE J. Struct. Div*. 100(ST1):11–29.

Wisniewski, B. and H. B. Manbeck. 2003. Residential floor systems: Wood I-joist creep behavior. *J. Architect. Eng*. 9(1):41–45.